

## THE IMAGINATION OF THE FORCED DRIVEN DISK-RIDGING TOOL AND IT'S WORKING PROCESS IN THE MATHCAD ENVIRONMENT

Heinloo, M & Olt, J.

### Abstract

This paper presents the mathematical modelling method to create of the video frames of the virtual projections of the forced driven disk-ridging tool, which is intended for earth up the potato ridges. Computer package Mathcad was used to make video clips with animations of motion of the virtual projections of the disk-ridging tool and to imagine of its working process. The imagined areas on the lateral side of the potato ridge, processed by the disk-ridging tool with different angular velocities are determined. The delving process of the blade of the disk-ridging tool into the soil has been studied in detail by use of the animation of motion of the virtual projections of the blade. Obtained knowledge is recommended to be used for making precise technical drawings for machine with disk-ridging tools. The results of this study are illustrated by several frames from the composed video clips.

Key words: *agriculture, machinery, technology, animation, potato field, video clip.*

### 1. INTRODUCTION

Essential aid to study and solve the practical problems of machinery is the use of mathematical and virtual models of machine elements and the imaginations of their working processes. World practice shows that the use of these models in study is often much cheaper and more effective than only a practical experimentation. Therefore, it is reasonable to start the experiments only after full study of the mathematical and the virtual models.

The disk-ridging tools can be used in the structures of the potato field ridging machines for earth up the potato ridges. The disk-ridging tool is called as free-active if it is driven only by the forces, applied to this tool in the soil. Olt, Reintam (1984) used the free-active disk-ridging tool in the structure of the new combine wide row potato field tillage machine. Olt, Heinloo (2002) reviewed the results of theoretical and experimental study of free-active tools of combine machine, named above.

Disk-ridging tool, driven by transmission from tractor, is called as forced driven disk-ridging tool, which rotates independently from the velocity of traversing the frame of the ridging machine.

This paper concentrates the main attention on the mathematical modelling method for creation the virtual projections of the disk-ridging tool on the Mathcad worksheet and for visualisation the motion of the forced driven risk-ridging tool and its working process on the lateral side of a potato ridge in the case of various angular velocities. The results of this paper have to be recommended for precise projection of the disk-ridging tools for potato field ridging machines

### 2. A DISK-RIDGING TOOL

The disk-ridging tool was considered as a disk of radius  $r$  with trapezoidal blades, clamped to it (Fig. 1), with an adjustment angle  $\xi$  to the radial direction of the disk. The trapezoidal

blades of the disk-ridging tool have width  $d$  and the angle of inclination  $\zeta$  to the plane of the disk of the disk-ridging tool. The disk-ridging tool has an angle of attack  $\alpha$  to the direction of its traversing and the angle of inclination  $\beta$  to the plane of the disk. In the structure of potato field ridging machines for earth up the potato ridges the disk-ridging tool has complex motion: it moves forward together with whole machine and rotates relatively to the frame of the machine.

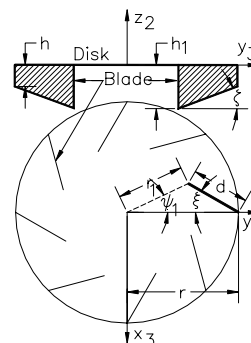


Fig. 1. The scheme of the disk ridging tool

Fig. 2 shows the ridging tool on the lateral surface of a ridge of a potato field in a working position. According to the agricultural engineering requirements the tolerance between the upper edges of the lateral surface of the potato ridge is  $\delta$  and the distance between the centre of disk and the lateral surface is  $H$ .

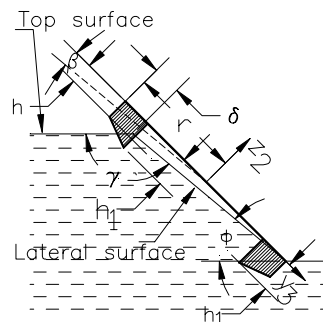


Fig. 2. The scheme of the ridging tool on a lateral surface of a potato field's ridge

### 3. DETERMINATION OF THE POSITIONS OF A DISK-RIDGING TOOL

For determination the positions of the disk-ridging tool the co-ordinate systems, shown in Fig. 3, were used. The motionless observation system  $Oxyz$  relative to the lateral surface of the potato ridge was used. The auxiliary co-ordinate system  $O_1x_2y_2z_2$  was supposed to be in forward motion together with the tool. Its position before motion is  $Ox_2y_2z_2$ . The orientation of the disk-ridging tool relative to the system  $Oxyz$  determines the rigidly connected to the tool co-ordinate system  $O_1x_3y_3z_2$

(Fig. 3). The position of the tool in the system Oxyz is determined by angle of attack  $\alpha$ , angle of inclination  $\beta$ , angle of rotation  $\varphi$ , distance between origins O and O<sub>1</sub>. Axes of the motionless co-ordinate system Oxyz are directed as follows. Axis Oz is perpendicular to the lateral surface of the ridge. Axis Oy is perpendicular to the axis Oz and directed to the permanent direction of motion of the machine, carrying the disk-ridging tool. Axis Ox is perpendicular to the axes Oz and Oy and forms together with these axes the rectangular right hand co-ordinate system.

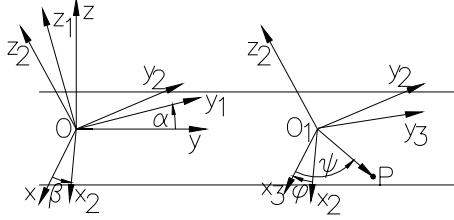


Fig. 3. The co-ordinate systems

The co-ordinates  $x, y, z$  of the point P (Fig. 3) in the co-ordinate system Oxyz are determined by the equality

$$\begin{bmatrix} x(\alpha, \beta, \varphi, r, \psi, z_2) \\ y(\alpha, \beta, \varphi, r, \psi, z_2, t) \\ z(\alpha, \beta, \varphi, r, \psi, z_2, H) \end{bmatrix} = A(\alpha)B(\beta)C(\varphi) \begin{bmatrix} x_3(r, \psi) \\ y_3(r, \psi) \\ z_2 \end{bmatrix} + \begin{bmatrix} 0 \\ v_m t \\ H \end{bmatrix}, \quad (1)$$

where

$$A(\alpha) = \begin{bmatrix} 1 & 0 & 0 \\ 0 & \cos(\alpha) & -\sin(\alpha) \\ 0 & \sin(\alpha) & \cos(\alpha) \end{bmatrix},$$

$$B(\beta) = \begin{bmatrix} \cos(\beta) & 0 & \sin(\beta) \\ 0 & 1 & 0 \\ -\sin(\beta) & 0 & \cos(\beta) \end{bmatrix}$$

$$C(\varphi) = \begin{bmatrix} \cos(\varphi) & \sin(\varphi) & 0 \\ -\sin(\varphi) & \cos(\varphi) & 0 \\ 0 & 0 & 1 \end{bmatrix},$$

$$x_3(r, \psi) = r \cos(\psi), \quad y_3(r, \psi) = r \sin(\psi)$$

$v_m$  – the velocity of the origin O<sub>1</sub> (machine);  $H$  – the distance between the lateral surface of the ridge and origin O<sub>1</sub>;  $r$  and  $\psi$  – polar radius and polar angle of the point P of the disk-ridging tool in the co-ordinate system O<sub>x<sub>3</sub>y<sub>3</sub>z<sub>2</sub></sub>.

#### 4. COMPOSITION OF VIDEO FRAMES

Let us compose the vector of the blade corner's co-ordinates

$$s_X(i, j) = \begin{pmatrix} X(\alpha, \beta, \varphi_i, r, \psi_j, -h) \\ X(\alpha, \beta, \varphi_i, r, \psi_j, 0) \\ X(\alpha, \beta, \varphi_i, r, \psi_j + \psi_{i,0}) \\ X(\alpha, \beta, \varphi_i, r, \psi_j + \psi_{i,-h_1}) \\ X(\alpha, \beta, \varphi_i, r, \psi_j, -h) \end{pmatrix} \quad (2)$$

where  $X = x, y, z$ ;  $h_1 = h + d \tan(\zeta)$ ,  $\psi_{i,0} = a \sin\left(\frac{d \sin(\xi)}{r_r}\right)$ ,

$$r_r = \sqrt{d^2 + r_1^2 - 2r_1 d \cos(\xi)} \quad \text{and} \quad \varphi_i = \frac{\omega T}{N} i, \quad \psi_j = \frac{\pi}{2} + \frac{2\pi}{M} j.$$

Here  $i = 0, 1, 2, \dots, N$ ;  $j = 0, 1, 2, \dots, M$ ;  $\omega$  – angular velocity of the disk-ridging tool,  $T$  – given interval of time,  $N$  – number of positions of the disk-ridging tool in the computations,  $M$  –

number of blades of the disk-ridging tool. By use of linear interpolation formula between of the corner points of a blade the contours of a blade can be obtained.

Figs. 4 – 6 show the first video frame of the virtual projection of the contour of the blade of number  $j = 0$  at the initial position ( $i = 0$ ) on the co-ordinate planes Oxy, Oxz, Oyz, when the disk-ridging tool has the following values of the parameters (Figs. 1, 3):  $\delta = 0.046$  m;  $h = 0.04$  m;  $d = 0.2$  m;  $\xi = 20^\circ$ ;  $\alpha = 8^\circ$ ;  $\beta = 5^\circ$ ;  $H = 0.043$  m;  $\zeta = 8^\circ$ ;  $T = 3$  s;  $N = 2000$ ;  $M = 8$ ;  $\omega = 16$  1/s, 12 1/s, 8 1/s;  $\pi = 3.1416$ ;  $r = 0.325$  m. The values of parameters  $H, \alpha, \beta, \zeta$  were chosen to satisfy the following conditions of agricultural engineering for disk-ridging tool:

1. the thickness of layer, to be processed, will be 0.05 m,
2. the angle between of the lateral side of the “ridge” (co-ordinate plane Oxy) on the lower edge of the blade is equal to zero, when the blade is parallel to the direction of traversing of the disk-ridging tool.

The hatching in Figs. 4 – 6 shows the regions to be processed.

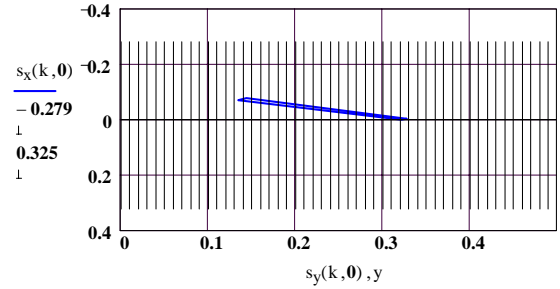


Fig. 4. First video frame of the virtual projection of the contour of the blade No 0 on the co-ordinate plane Oxy at the initial position

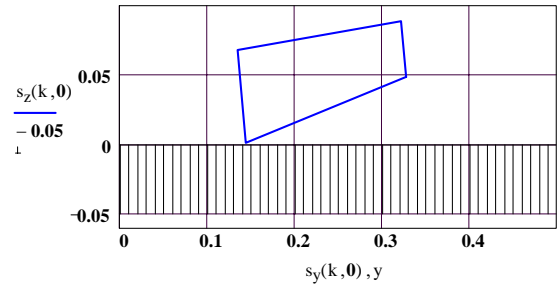


Fig. 5. First video frame of the virtual projection of the contour of the blade No 0 on the co-ordinate plane Oyz at the initial position

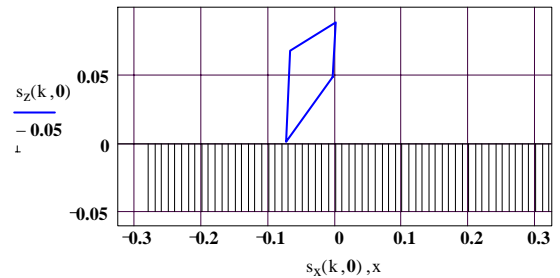


Fig. 6. First video frame of the virtual projection of the contour of the blade No 0 on the co-ordinate plane Oxz at the initial position

Let us compose the new vector by putting the vector  $s_X(i+1, 0)$  upon the vector  $s_X(i, j)$  ( $X = x, y, z$ ). The Mathcad programs

$$S'_x(i) := \begin{cases} S_x \leftarrow s_x(i, 0) \\ \text{for } j \in 1 \dots M \\ S_x \leftarrow \text{stack}(S_x, s_x(i, j)) \end{cases}$$

$$S'_y(i) := \begin{cases} S_y \leftarrow s_y(i, 0) \\ \text{for } j \in 1 \dots M \\ S_y \leftarrow \text{stack}(S_y, s_y(i, j)) \end{cases}$$

$$S'_z(i) := \begin{cases} S_z \leftarrow s_z(i, 0) \\ \text{for } j \in 1 \dots M \\ S_z \leftarrow \text{stack}(S_z, s_z(i, j)) \end{cases}$$

do this procedure. Vectors  $S'_x(i)$ ,  $S'_y(i)$ ,  $S'_z(i)$  contain the corner's  $x$ ,  $y$ ,  $z$  co-ordinates of all blades accordingly. By joining these points by lines the virtual projections of all blades together with an auxiliary polygon can be composed.

For here considered case the parameters of the first video frame of virtual projections of all blades together with the auxiliary polygon are shown in Figs. 7 – 9 at the beginning of motion.

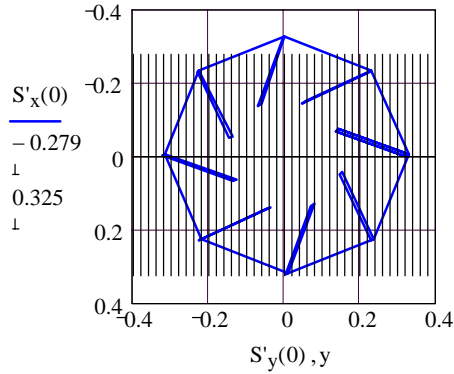


Fig. 7. First video frame of virtual projections of all blades on plane  $Oxy$  at the beginning of motion.

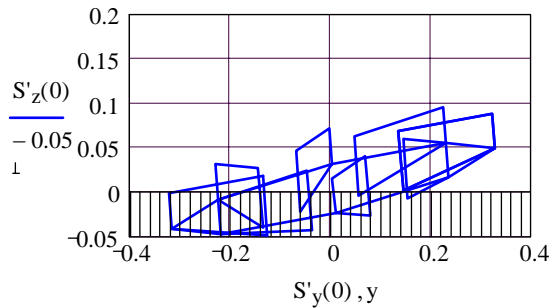


Fig. 8. First video frame of virtual projections of all blades on plane  $Oyz$  at the beginning of motion.

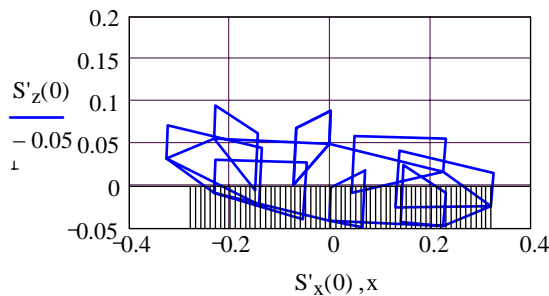


Fig. 9. First video frame of virtual projections of all blades on plane  $Oxz$  at the beginning of motion.

Let us compose the new vector by putting the vector  $s_x(0, j+1)$  upon the vector  $s_x(i, j)$  ( $X = x, y, z$ ). The Mathcad programs

$$S_x(j) := \begin{cases} S_x \leftarrow s_x(0, j) \\ \text{for } i \in 1 \dots N \\ S_x \leftarrow \text{stack}(S_x, s_x(i, j)) \end{cases}$$

$$S_y(j) := \begin{cases} S_y \leftarrow s_y(0, j) \\ \text{for } i \in 1 \dots N \\ S_y \leftarrow \text{stack}(S_y, s_y(i, j)) \end{cases}$$

$$S_z(j) := \begin{cases} S_z \leftarrow s_z(0, j) \\ \text{for } i \in 1 \dots N \\ S_z \leftarrow \text{stack}(S_z, s_z(i, j)) \end{cases}$$

do this procedure. Vectors  $S_x(j)$ ,  $S_y(j)$ ,  $S_z(j)$  contain the corner's  $x$ ,  $y$ ,  $z$  co-ordinates of  $j$ -th blade in all positions, accordingly. By joining these points by lines the virtual image of processed part of the lateral surface of a potato ridge can be composed.

## 5. DENSITY OF PROCESSED AREA ON THE LATERAL SURFACE OF A POTATO RIDGE

By use of the functions  $S_x(j)$ ,  $S_y(j)$ ,  $S_z(j)$  the virtual images of areas on the lateral surface of a potato ridge (co-ordinate plane  $Oxy$ ), processed with the various angular velocities of the disk-ridging tool with 8 blades, are obtained.

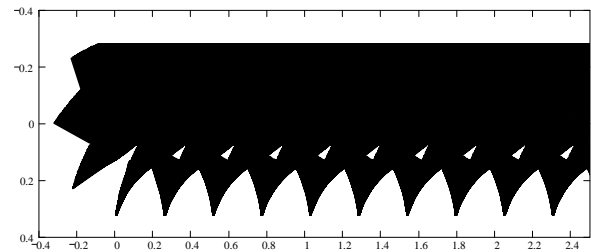


Fig. 10. Virtual image of the area, processed by the virtual disk-ridging tool on lateral surface of a ridge (co-ordinate plane  $Oxy$ ) with angular velocity  $\omega = 8$  1/s and traversing velocity 2.6 m/s.

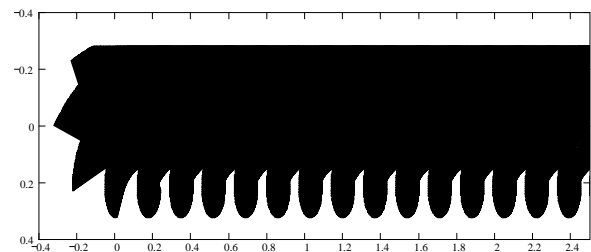


Fig. 11. Virtual image of the area, processed by the virtual disk-ridging tool on lateral surface of a ridge (co-ordinate plane  $Oxy$ ) with angular velocity  $\omega = 12$  1/s and traversing velocity 2.6 m/s.

Figs. 10 – 12 show the density of virtual images of the processed areas, considered in this paper parameters of the disk-ridging tool, when it moves from left to the right in Figs 10 - 12 with the velocity  $v_m = 2.6$  m/s of traversing and rotates with forced angular velocities  $\omega = 8$  1/s (Fig. 10),  $\omega = 12$  1/s (Fig. 11),  $\omega = 16$  1/s (Fig. 12). It turned out from Figs. 10 – 12

that the density of processing depends substantially from the angular velocity of rotation of the disk-ridging tool. Fig. 12 shows that the disk-ridging tool with 8 blades, working with angular velocity  $\omega = 16$  1/s and traversing with velocity 2.6 m/s gives sufficient density of processing the lateral surface of a ridge. Thus these velocities can be recommended for designers of the potato field ridging machines.

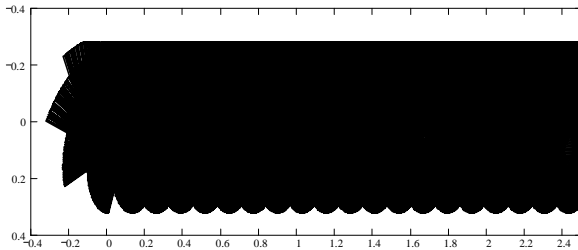


Fig. 12. Virtual image of the area, processed by the virtual disk-ridging tool on lateral surface of a ridge (co-ordinate plane Oxy) with angular velocity  $\omega = 16$  1/s and traversing velocity 2.6 m/s.

## 6. CREATION OF VIDEO CLIPS

By using the composed video frames of the disk-ridging tool and the parameter  $i$ , which determine the  $i$ -th frames, the motion of the virtual projections can be animated, if the parameter  $i$  is changeable after certain interval of a time.

The video clips were composed in the environment of computer package Mathcad, which has the special built in parameter FRAME for animation. The value of parameter FRAME changes after every set value of time and can be assigned to the parameter  $i$  for animation.

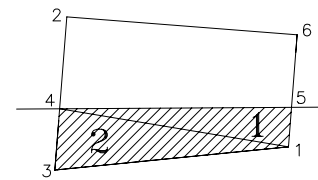
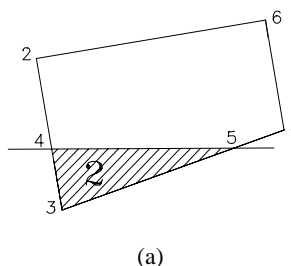
The video clips “Motion of the blade.avi”, “Motion of the disk-ridging tool.avi” and “Processing.avi” with animations of the virtual projections of the disk-ridging tool have been composed by the first author of this paper.

## 7. DETAIL STUDY THE VIRTUAL DELVING PROCESS OF THE BLADE INTO A RIDGE

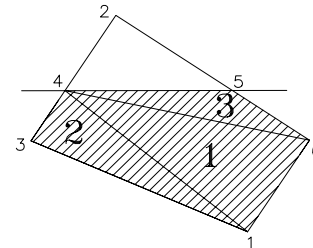
For study hereafter the forces, applied to the delved part of the blades of the disk-ridging tool the detail know-how on the delving process of this blade into the soil is needed.

Let us assume, that the disk-ridging tool moves forward together with ridging machine with the velocity of  $v_m = 2.6$  m/s. The video clip “Motion of the blade.avi” can be used for detail analysis of the delving process of the blade into the soil.

In the case, considered in this paper parameters, the video clip “Motion of the blade.avi” shows that a blade has three typical positions in the process of delving into a ridge, shown in Fig. 10. Firstly delves into a ridge the corner point 3 of the blade. Then, during some time, the delved part of the blade has the triangular form (Fig. 13a). After delving the corner point 1 into the ridge the delved part of the blade changes to the tetragonal form (Fig. 13b). Finally, after delving the point 6 of the blade into the ridge the delved part changes to pentagon form (Fig. 13c). The blade leaves the ridge on the opposite order.



(b)



(c)

Figure 13. The delving process of a blade into the ridge

## 8. ON USAGE OF THE REST OF THE VIDEO CLIPS

The video clips “Motion of the disk-ridging tool.avi” and “Motion of the blade.avi” allow to control the satisfaction of the agricultural engineering conditions, applied to the disk-ridging tool. The video clip “Processing.avi” can be used to visualise the process of virtual processing of the lateral surface of a potato “ridge” and to control the quality of processing.

## 9. CONCLUSION

Mathematical modelling method, used in this paper to create video frames for animation the motion of the virtual projections of the machine elements can also used to obtain useful information for experimental study of various machines, their elements and working processes. Our experience shows that the computer package Mathcad has the convenient environment for mathematical modelling and imagination of various tools and their working processes.

## 10. REFERENCES

- Olt, J., Reintam, A. (1984) Certificate of author SU – 1130182.
- Olt, J.; Heinloo, M. (2002) On Know-How for Creating a New Sustainable Combine Wide Row Potato Field Tillage Machine. Proc. 3<sup>rd</sup> Int Conf. Industrial Engineering – New Challenges to SME, Tallinn, pp. 42 – 45.

## ACKNOWLEDGEMENT

The authors are grateful to the Estonian Science Foundation for their support (Grant No. 4098).